Journal of Structural Geology, Vol. 12, No. 8, pp. 1033 to 1045, 1990
Printed in Great Britain

0191-8141/90 $03.00+0.00

Shear zones developed in an experimentally deformed quartz mylonite

STEVEN RALSER*

Department of Earth Sciences, Monash University, Clayton, Victoria, 3168, Australia

(*Received* 6 *June* 1989; *accepted in revised form* 15 *March* 1990)

Abstract—Specimens of an experimentally deformed quartz mylonite show the development of shear zones. These shear zones are of two types: Type A shear zones are discrete and within the specimen, whereas Type B shear zones occur where the specimen has been sheared past the corner of the piston. Type A shear zones are comprised of elongate recrystallized grains with long axes oriented 30–40° to the shear zone boundary. Type B shear zones consist of strongly flattened and recrystallized ribbon grains. Augen occur where the deformation history is coaxial; around the piston corner where the deformation history is non-coaxial only strongly flattened grains occur. The *c*-axis fabrics which develop in the shear zones comprise girdles or maxima approximately normal to the foliation defined by the grain elongation (shape fabric). An asymmetry with respect to the shape fabric is present in many of the fabrics. This asymmetry results from either using a quartz mylonite with a strong preferred orientation as the starting material, or as a result of the non-coaxial deformation. Where it can be demonstrated that the asymmetry results from the non-coaxial deformation, the asymmetry is a leading edge with respect to the sense of shear. The results of this study suggest that care must be taken in interpreting asymmetric quartz *c*-axis fabrics in natural shear zones, particularly if it is suspected that the protolith to the shear zone had an initially strong preferred orientation.

Type A shear zones originate as brittle zones extending from the specimen corners, which become recrystallized as pressure and temperature are increased. These shear zones show initial non-coaxial deformation (dominantly simple shearing), followed by later flattening parallel to the shortening direction. Type B shear zones form when the piston punches into the barreling specimen. The strain history of these shear zones is characterized by initial flattening (up to 30%), followed by shearing past the piston corner.

INTRODUCTION

DEFORMATION within the Earth's crust is commonly found to be heterogeneous and localized in narrow zones where a non-coaxial strain history dominates (i.e. the axes of incremental and finite strain do *not* coincide throughout the deformation history). Such zones are termed shear zones and occur in crystalline basement rocks throughout the world (Ramsay 1980, 1983). Given similar rock types, the microfabrics (both the microstructures and crystallographic preferred orientations) of such zones are remarkably similar, pointing to similar deformation conditions and mechanisms. It is through a combination of field, experimental and theoretical studies that these conditions and mechanisms can be determined. Distinctive asymmetric quartz *c*-axis preferred orientations are commonly observed in such shear zones. An important question is whether we can relate the sense of asymmetry in the *c*-axis preferred orientation to the sense of shear of the shear zone. Shear zones have been observed in a number of experimentally deformed quartz mylonite specimens (Ralser 1987, Ralser *et al.* 1987), and form the basis of the present paper. This research also investigates the effect that an initial strong preferred orientation has on the asymmetry of the developed *c*-axis fabric in the shear zones.

Experimental studies designed to reproduce shear zones in aggregates of common rock-forming minerals (quartz, calcite and olivine) are rare, being confined primarily to calcite (Rutter & Rusbridge 1977, Friedman & Higgs 1981, Kern & Wenk 1983, Schmid *et al.* 1987). Tullis (1977) obtained a non-coaxial deformation history where the edge of the specimen sheared past the piston. Dell'Angelo & Tullis (1989) deformed thin slices of quartzite in simple shear. These experimental studies as well as those described in the present paper show many features which are also observed in natural shear zones.

The microstructure developed in quartz aggregates during non-coaxial deformation histories are a function of both the deformation conditions and the shear strain. At deformation conditions where recrystallization is limited, grains become elongate and ribbon-like parallel to the finite extension direction with increasing shear strain. Undeformed augen are not preserved because grains in strong orientations spin with respect to the instantaneous strain axes until oriented in a weak direction (e.g. Tullis *et al.* 1973). The crystallographic preferred orientations which develop comprise *c*-axis girdles approximately normal to the shear plane, with an *a*-axis maximum normal to this girdle, parallel to the shear direction (Schmid & Casey 1986). Such detailed studies suggest that deformation is accommodated solely by dislocation slip on the basal, prism, and rhomb planes in the ⟨*a*⟩ direction (Bouchez & Pêcher 1978, Schmid & Casey 1986). The *c*-axis girdles are asymmetric with respect to the shape fabric (foliation defined by the grain elongation). The asymmetric pattern indicates a non-coaxial strain history, while the direction of asymmetry with respect to the shape fabric reflects the sense

*Present address: Centre for Deformation Studies in the Earth Sciences, Department of Geology, University of New Brunswick, Fredericton, NB, Canada E3B 5A3.

of shear (see compilation by Price 1985). Variations within this fabric pattern are usually explained by differences in deformation conditions.

In summary, natural shear zones are characterized by elongate, flattened grains. No augen are preserved as slip systems spin with respect to the deformation axes. *c*-axes form girdles which remain approximately normal to the shear plane. The sense of asymmetry of the *c*-axis girdle with respect to the shape fabric can be used to determine the sense shear of the shear zone.

EXPERIMENTAL PROCEDURE

The experiments described in this paper were not designed specifically to examine shear zone development. The experiments were set up to study the influence of a strong preferred orientation on strength of the specimen, developed microstructures and *c*-axis preferred orientation (Ralser *et al.* 1987, and work in preparation). Shear zones developed because at high strains the piston tends to punch through the specimen.

The starting material was a pure quartz mylonite (with minor mica), consisting of equant grains, with an approximate mean grainsize of 0.2 mm, but ranging up to 0.4 mm (Fig. 1), and an asymmetric Type I *c*-axis girdle (Lister 1977), normal to the mylonitic foliation and lineation (Fig. 2). The mylonitic foliation is defined by changes in grainsize and changes in the proportion of mica present; the lineation is defined by mica. This mylonite was collected from a shear zone at Little Broken Hill, near Broken Hill, New South Wales, Australia. It was originally a quartz pegmatite, now strongly deformed in the shear zone. Specimens were deformed in the laboratory in four orientations relative to the mylonitic foliation and lineation, but only two orientations will be discussed in this paper (Fig. 2); PSL, parallel to the foliation and lineation, and NSL, normal to the foliation and lineation. The experimental procedures are similar to those used by Ord & Hobbs (1986). Experiments were conducted in a Tullis-modified Griggs deformation apparatus, using NaCl as the confining medium. Specimens (either 12 or 15 mm long and 6.45 mm in diameter) were encapsulated in either nickel or silver, with 50 μl water added. The specimens described here were deformed at temperatures of 700–800°C, strain rates of 10^{-5} and 10^{-6} s^{-1}, and a confining pressure of 1.64 GPa, with shortening of up to 65% (Table 1). The chemical environment is buffered at either an oxygen fugacity of 10^{-31} MPa (Ta–Ta_2O_5 buffer added with water in a silver jacket; Ord & Hobbs 1986) or 10^{-15} Mpa (water added in a nickel jacket; Davidson personal communication 1986). These experimental conditions are such that recrystallization is limited, with strain accommodated primarily by plastic deformation. The experimental procedure used in the experiments described in this paper differ from those used by Ord & Hobbs (1986) in two ways: (a) nickel capsules, without added buffers, are used in all but one of the experiments, and (b) the specimens were kept at pressure and temperature for between 20 and 30 h prior to the initiation of deformation.

Crystallographic preferred orientations were measured using the photometric technique (Price 1979), using, in most cases, the highest powered objective available (32 ×). Where the shear zones were too narrow to use the photometer, the gypsum plate was used to give an indication of *c*-axis distribution with respect to the recrystallized grain elongation within the shear zones. The grainsize in the shear zones is too small to allow measurement of individual grain orientations.

STRENGTH OF THE SPECIMENS

Stress–strain curves are shown for the four specimens deformed to high strains (Fig. 3). At these experimental conditions specimens deformed PSL are weaker than specimens deformed NSL (Ralser 1987, Ralser *et al.* 1987). All specimens are characterized by a peak stress (dependent on specimen orientation and deformation conditions) between strains of 9% and 15%, followed by strain softening. In the extreme this softening is down to 30% of the peak stress (G0251, Fig. 3). Specimen G0251 (Fig. 3) shows an anomalously high stress for the deformation conditions (800°C, 10^{-5} s^{-1}). The reason for this is unknown. The increase in stress at high strains (>30%) in this experiment results from failure of the furnace and/or thermocouple.

MICROSTRUCTURE

Two different types of shear zones occur (Fig. 4): *Type A shear zones* are discrete and cut through the specimen at approximately 45–60° to the shortening direction, and *Type B shear zones* occur at the edges of the specimen where it has been sheared past the corner of the piston. These names are used here to distinguish the shear zones for descriptive purposes only. No microstructural differences due to the different initial orientations of the specimens are observed.

Type A shear zones (Figs. 5 and 6)

Type A shear zones occur in both comparatively undeformed and highly deformed specimens. The shear zones are developed best in three specimens, one shortened PSL (G0297, 800°C, 10^{-6} s^{-1}, $\varepsilon = 27\%$) and two shortened NSL (G0342, 700°C, 10^{-6} s^{-1}, $\varepsilon = 60\%$; G0227, 700°C, 10^{-6} s^{-1}, $\varepsilon = 53\%$). The shear zones are up to 200 μm wide, and are inclined between 45° and 60° to the shortening direction. The boundaries of the shear zones are irregular, either wrapping around surrounding grains, or cutting across grains (Fig. 5d). In the less deformed specimen (G0297, Figs. 5a & b) grains surrounding the shear zone are comparatively undeformed, showing only minor flattening normal to the shortening direction. At higher strains the surrounding grains show greater flattening (Figs. 5c & d and 6).

The shear zones are characterized, optically, by

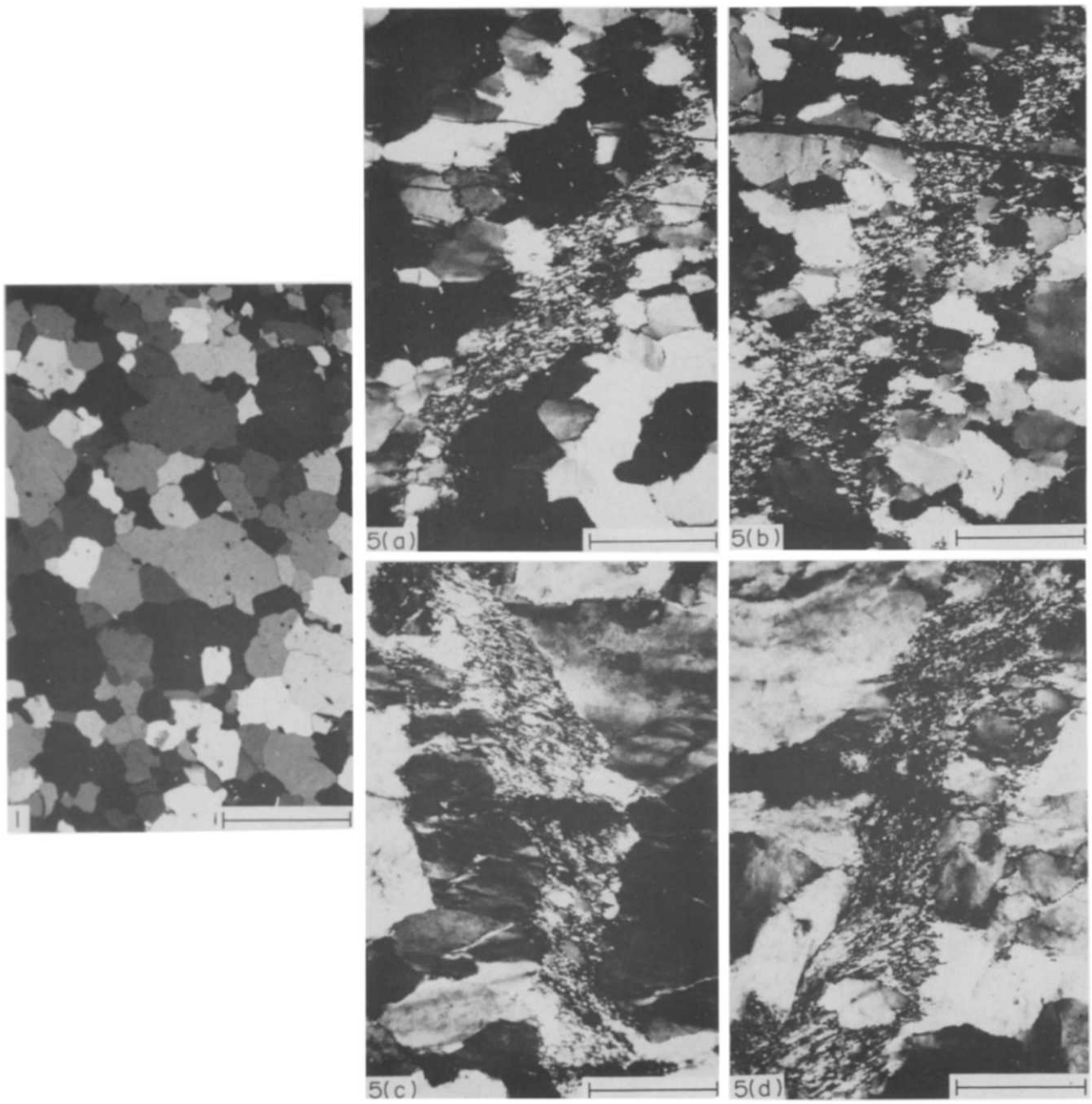

Fig. 1. Initial microstructure of quartz mylonite (foliation and lineation E–W). Scale bar = 200 μm.

Fig. 5. Type A shear zones developed through low strained host grains. (a) & (b) in G0297 (PSL, 800°C, 10^{-6} s^{-1}, ε = 27%); (c) & (d) in G0227 (NSL, 700°C, 10^{-6} s^{-1}, ε = 53%). Scale bar = 200 μm. All photomicrographs have the shortening direction N–S.

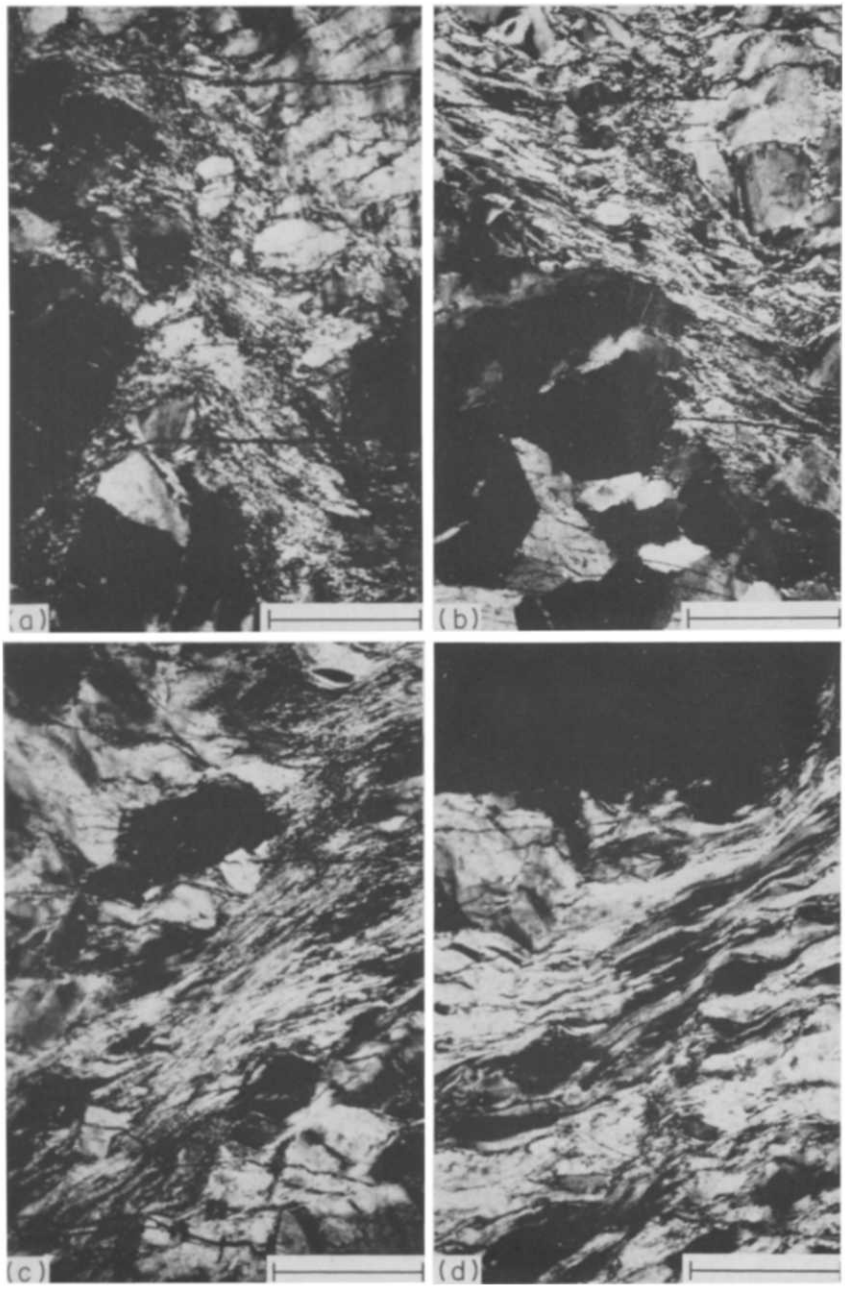

Fig. 6. Type A shear zones developed in G0342 (NSL, 700°C, 10^{-6} s^{-1}, ε = 49%). (a)–(c) Shear zones with recrystallization; (d) shear zones showing only plastically deformed grains. Scale bar = 200 μm.

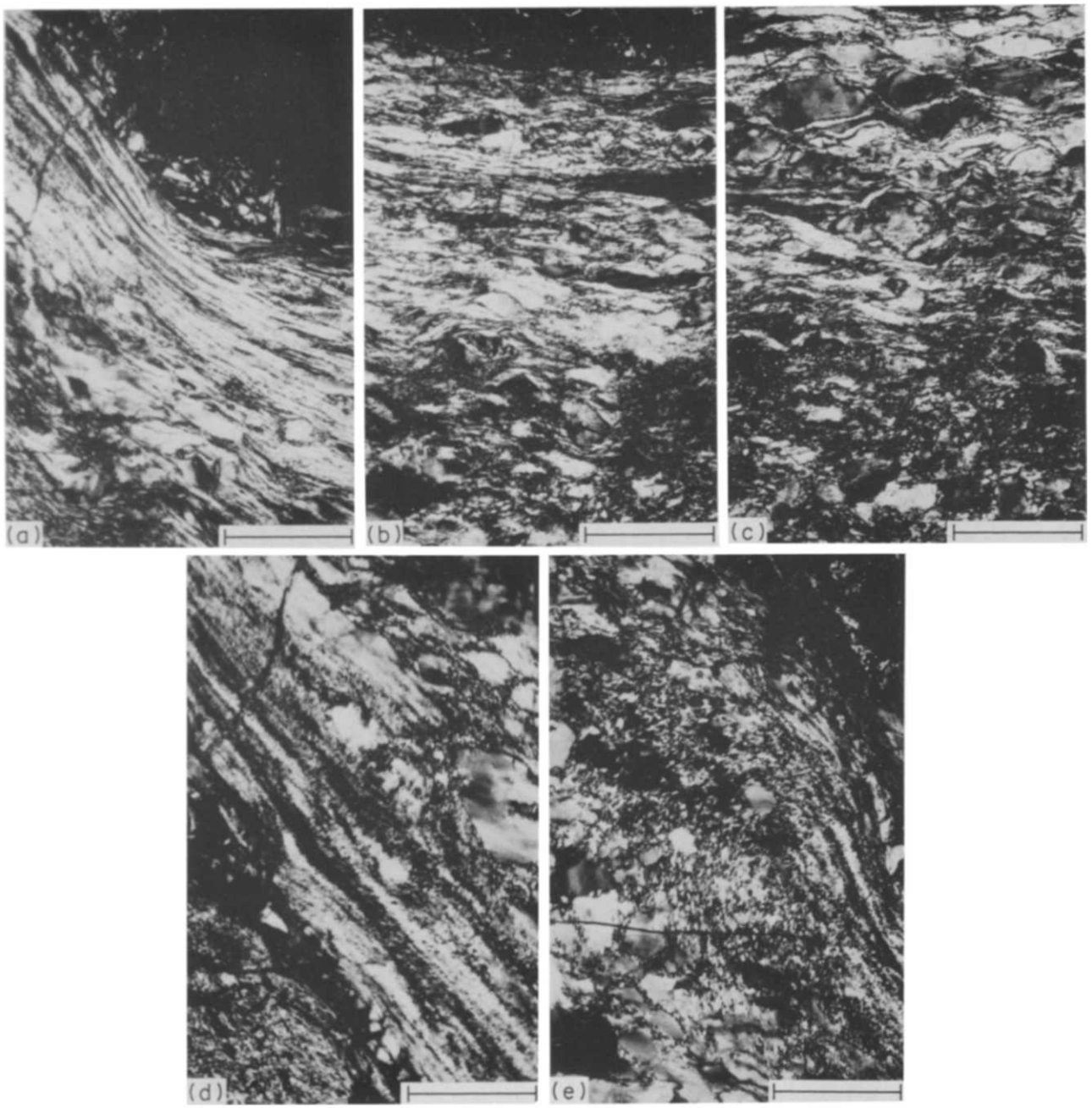

Fig. 7. Microstructures of Type B shear zones developed across the top of G0251 (PSL, 800°C, 10^{-5} s^{-1}, $\varepsilon = 57\%$). The component of non-coaxial deformation decreases from (a)→(b)→(c). (d) Ribbon grains showing the development of subgrains on the side of the piston; (c) complex foliation to the side of the piston. The location of the photomicrographs is shown on the outline of the specimen section in Fig. 12. Scale bar: (a)–(c) & (e) = 200 μm, (d) = 50 μm.

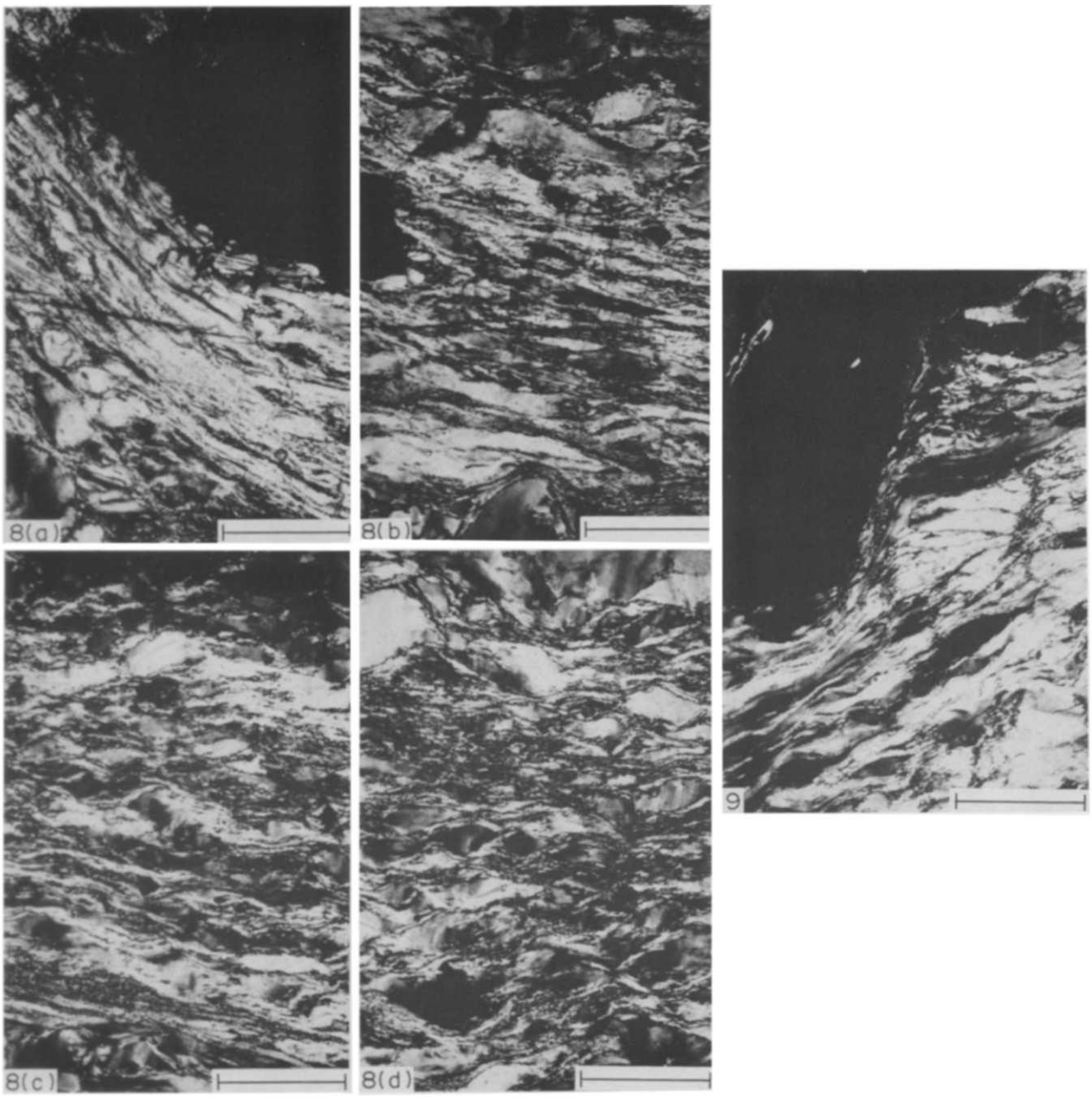

Fig. 8. Microstructures of Type B shear zones developed across the top of G0263 (NSL, 800°C, 10^{-6} s^{-1}, Ta buffer, $\varepsilon = 64\%$). In (a) the deformation history is dominantly non-coaxial, while in (d) the deformation history is essentially coaxial. The coaxial deformation history is indicated by the foliation approximately normal to the shortening direction, and the abundant comparatively undeformed augen. The location of the photomicrographs is shown on the outline of the specimen section in Fig. 13. Scale bar = 200 μm.

Fig. 9. Type B shear zone developed in specimen G0342 (NSL, 700°C, 10^{-6} s^{-1}, $\varepsilon = 49\%$), to the top right of the Type A shear zone illustrated in Fig. 6(d). Scale bar = 200 μm.

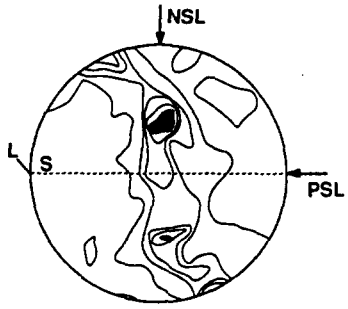

Fig. 2. Initial *c*-axis preferred orientation of quartz mylonite; orientations of the specimens used in this study are indicated (PSL—parallel to the foliation (*S*) and lineation (*L*); NSL—normal to the foliation and lineation). *c*-axes measured manually on the universal stage; 200 grains, contours 0.5, 2 and 4% per 1% area, equal-area projection.

elongate recrystallized grains with long axes oriented 30–40° to the shear zone boundary (Figs. 5 and 6). The orientation of the elongate grains with respect to the shortening direction varies with the total strain of the specimen. G0297 (shortened 27%, Figs. 5a & b) has elongate grains at approximately 80° to the shortening direction. In the higher strained G0227 (Figs. 5c & d) and G0342 (Fig. 6), the grain elongation in the shear zones is at a lower angle to the shortening direction (up to 50° in G0342, Fig. 6c). One shear zone in G0342 (Fig. 5d) is comprised of only elongate grains with no recrystallization.

Type B shear zones (Figs. 7 and 8)

The most spectacular examples of shear zones in these experimentally deformed specimens occur where material is wrapped around the corners of the pistons. In these specimens the zone of non-coaxial deformation is marked by an area where the foliation is not normal to the shortening direction, and is concentrated in the region of the corner of the piston (e.g. G0251, shortened PSL, deformed at 800°C and a strain rate of $10^{-5}\,s^{-1}$, Fig. 7, with the location of the photomicrographs in the specimen section shown in Fig. 12), or extending under most of the piston (e.g. G0263, shortened NSL, deformed at 800°C and a strain rate of $10^{-6}\,s^{-1}$, Fig. 8, with the location of the photomicrographs in the specimen section shown in Fig. 13).

The deformed portion of these specimens includes only a small region with a shape fabric normal to the shortening direction (F0251 Figs. 7b & c; G0263, Fig. 8d). Such areas are characterized by both grains elongate normal to the shortening direction and equant augen. In the remainder of the deformed area, the shape fabric is at an angle to the shortening direction. The angle between the shape fabric and the overall shortening direction decreases across the top of the specimen towards the corner of the piston (G0251, Figs. 7a & b; G0263, Figs. 8b & c), before making a sudden change in angle around the corner of the piston (G0251, Fig. 7a; G0263, Fig. 8a). This is accompanied by a decrease in the number of augen (G0251, Figs. 7a–c; G0263, Fig. 8). Under the corner and up the side of the piston (G0251, Figs. 7a & d; G0263, Fig. 8a), all grains are ribbon-like, with no augen. In specimen G0251 these ribbon grains are recrystallized (Fig. 7d), and next to the piston, near the top of the specimen, a complex foliation pattern is developed (Fig. 7e).

A small Type B shear zone is developed in one corner of specimen G0342 (Fig. 9), to the top right of the Type A shear zone shown in Fig. 5(d). This shows strongly flattened grains to the right of the piston, some of which can be followed into elongate grains which have been sheared past the piston corner. A number of the elongate sheared grains can be followed around the piston corner.

The microstructures in both Types A and B zones are characterized by a foliation, defined by the grain elongation, inclined to the normal to the bulk shortening direction. Some of the larger relic grains in the shear zones show sub-basal deformation lamellae. In regions where the foliation is at a low angle (<60°) to the bulk shortening direction, ribbon grains with few comparatively undeformed augen develop. In areas where the foliation is at high angles to the bulk shortening direction (60–90°) the number of ribbon grains decreases, and the number of comparatively undeformed augen increases.

CRYSTALLOGRAPHIC PREFERRED ORIENTATIONS

Type A shear zones

Shear zones in specimens G0227 and G0297 are too narrow to allow measurement of the *c*-axis fabric using the photometric method. Analysis with the gypsum plate, however, shows a strong *c*-axis concentration approximately normal to the shape fabric.

The shear zones developed in specimen G0342 (Fig.

Table 1. Experimental conditions for specimens showing shear zones

Strain rate ($\log s^{-1}$)	Temperature (°C)	Orientation*	Confining pressure (MPa)	Jacket material	Buffer	% Strain†	Maximum strain‡	Run No.
−5	800	PSL	1650	Ni		57	93	G0251
−6	700	NSL	1525	Ni		53	64	G0227
	700	NSL	1600	Ni		49	64	G0342
	800	PSL	1680	Ni		27	27	G0297
	800	NSL	1680	Ag	$Ta–Ta_2O_5$	64	78	G0263

*PSL—shortened parallel to the foliation and lineation; NSL—shortened normal to the foliation and lineation.
†% strain is the average shortening of the specimen.
‡Maximum strain is the maximum measured longitudinal strain (% shortening).

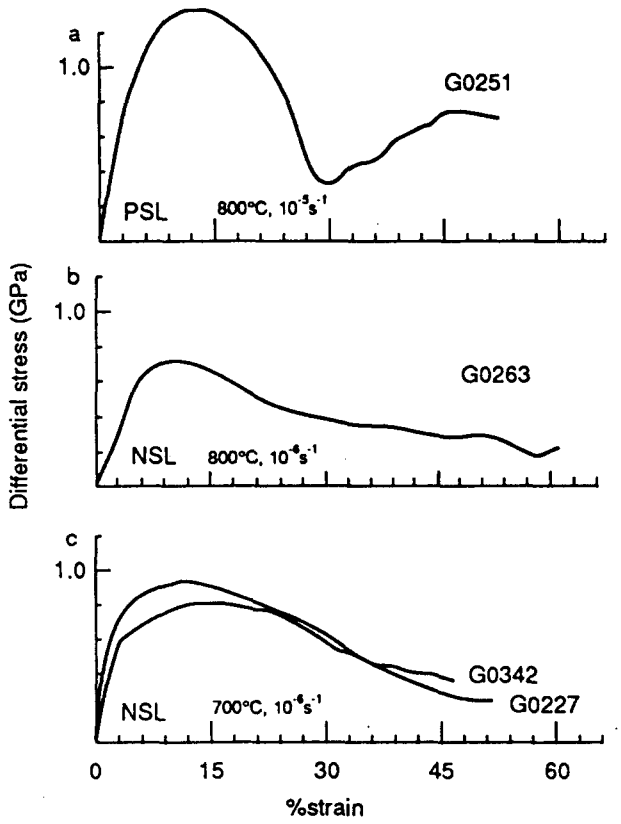

Fig. 3. Stress–strain curves for the four specimens which are shortened to high strains. (a) G0251 (PSL, 800°C, 10^{-5} s^{-1}, $\varepsilon = 57\%$); (b) G0263 (NSL, 800°C, 10^{-6} s^{-1}, Ta buffer, $\varepsilon = 64\%$; (c) G0342 (NSL, 700°C, 10^{-6} s^{-1}, $\varepsilon = 49\%$) and G0227 (NSL, 700°C, 10^{-6} s^{-1}, $\varepsilon = 53\%$).

10) are wide enough to be measured with the highest powered objective. The fabrics (Figs. 10a–d, corresponding to the shear zones shown in Fig. 6) show a well-developed girdle normal to the shape fabric. In addition, to a variable extent, the fabrics also show a maximum parallel to the shortening direction. No significant asymmetry is apparent with respect to the shape fabric. However, if the shear plane is taken as the reference plane, a trailing edge asymmetry (Fig. 11), with respect to the sense of shear, is observed.

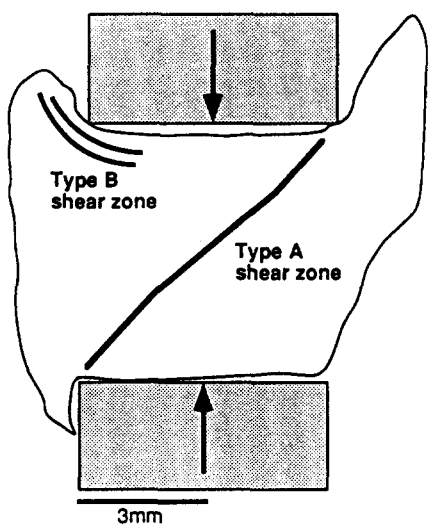

Fig. 4. Sketch showing outline of a hypothetical specimen with distribution of Type A and Type B shear zones marked. Pistons are shaded, and arrows indicate the shortening direction.

Type B shear zones

In Type B shear zones fabric development can be followed from areas under the centre of the piston, showing a coaxial deformation history, to areas around the side of the piston, showing a non-coaxial deformation history. The basic pattern which develops is similar to that developed in the Type A shear zones, namely a girdle approximately normal to the shape fabric, with a secondary maximum parallel to the shortening direction.

The *c*-axis fabrics measured in the areas showing a coaxial deformation history (fabrics M, S in G0251, Fig. 12; fabrics E,F,G in G0263, Fig. 13) are symmetrical with respect to both the shape fabric and the deformation axes. Towards and around the corner of the piston the fabrics form distinct girdles (Figs. 12 and 13) approximately normal to the foliation, remaining approximately normal as the foliation curves around the corner of the piston (follow fabrics F→G→N→H→O→P in Fig. 12; fabrics G→D→I→H in Fig. 13). The strongest fabrics develop around the corner of the piston, where the shear strain is concentrated (e.g. fabrics N,H in Fig. 12). In specimen G0251 fabric Q (Fig. 12), at the top of the specimen, shows a complex *c*-axis pattern, reflecting the complex foliation pattern (Fig. 7e), and therefore the complex strain history of this region.

The *c*-axis girdles are not always exactly normal to the shape fabric. In these cases, using the foliation as a reference plane (e.g. fabrics F,G,H,N,O in G0251, Fig. 12; fabrics H,I in G0263, Fig. 13) the sense of asymmetry defines a leading edge fabric (Fig. 11) with respect to the sense of shear.

In summary, *c*-axis girdles or maxima develop approximately normal to the foliation defined by the grain elongation. Fabrics measured in areas showing a non-coaxial deformation history often show an asymmetry with respect to the foliation. This asymmetry is a leading edge when the foliation defined by the shape fabric is used as a reference plane. However, in specimens where the shear zone boundary can be used as a reference plane the asymmetry can be described as a trailing edge.

DISCUSSION

Formation of the shear zones

Type A shear zones are characterized by narrow, non-planar recrystallized zones extending diagonally across the specimen from the sample corners. These originated as brittle fractures during pressurization, and subsequently became recrystallized as the temperature was increased (personal communication by anonymous reviewer). The recrystallized zones lie near the bound-

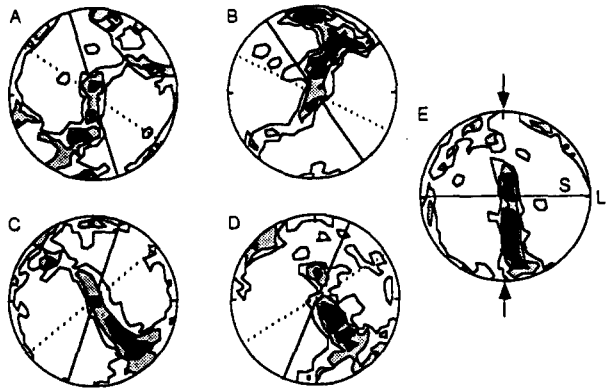

Fig. 10. *c*-axis fabrics developed in G0342 (NSL, 700°C, 10^{-6} s^{-1}, $\varepsilon = 49\%$). (a)–(d) Fabrics measured in the shear zones illustrated in Fig. 5(a)–(d), respectively. The dotted line indicates the orientation of the grain elongation, and the solid line indicates the orientation of the shear zone boundary. (e) *c*-axis fabric developed in centre of specimen, where the deformation history is coaxial; the initial orientation of the foliation (*S*) and lineation (*L*) is marked; the arrrows indicate the shortening direction. Contour interval 0.67, 2 and 4% per 0.67% area, based on 150 orientations; equal-area projection.

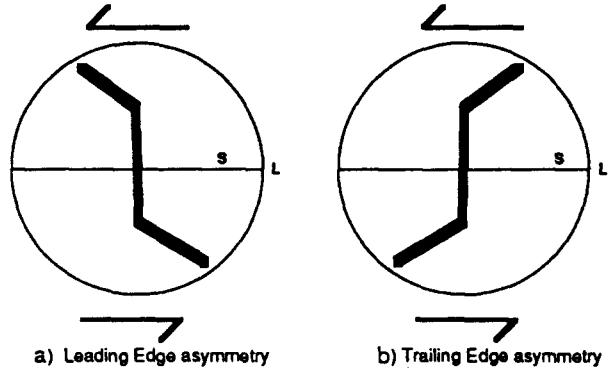

Fig. 11. Asymmetric *c*-axis preferred orientation showing (a) leading edge asymmetry with respect to the sense of shear and (b) trailing edge asymmetry with respect to the sense of shear.

ary of the 'dead zone' under the piston (an area which is not deforming because it is bounded by a non-slip contact with the piston). Differential movement between the 'dead zone' and the remainder of the specimen is initially localized in this recrystallized zone. At low strains most of the shortening is accommodated in such zones. This is illustrated in G0297 (Figs. 5a & b), with a total shortening of 27%, showing a recrystallized shear zone, with a grain elongation at approximately 80° to the shortening direction, contained within host grains which show only moderate deformation.

At higher strains host grains to the shear zones show greater effects of the deformation (Figs. 5c & d and 6), suggesting a component of axial shortening in the shear zones in addition to shearing. The elongate fabric at

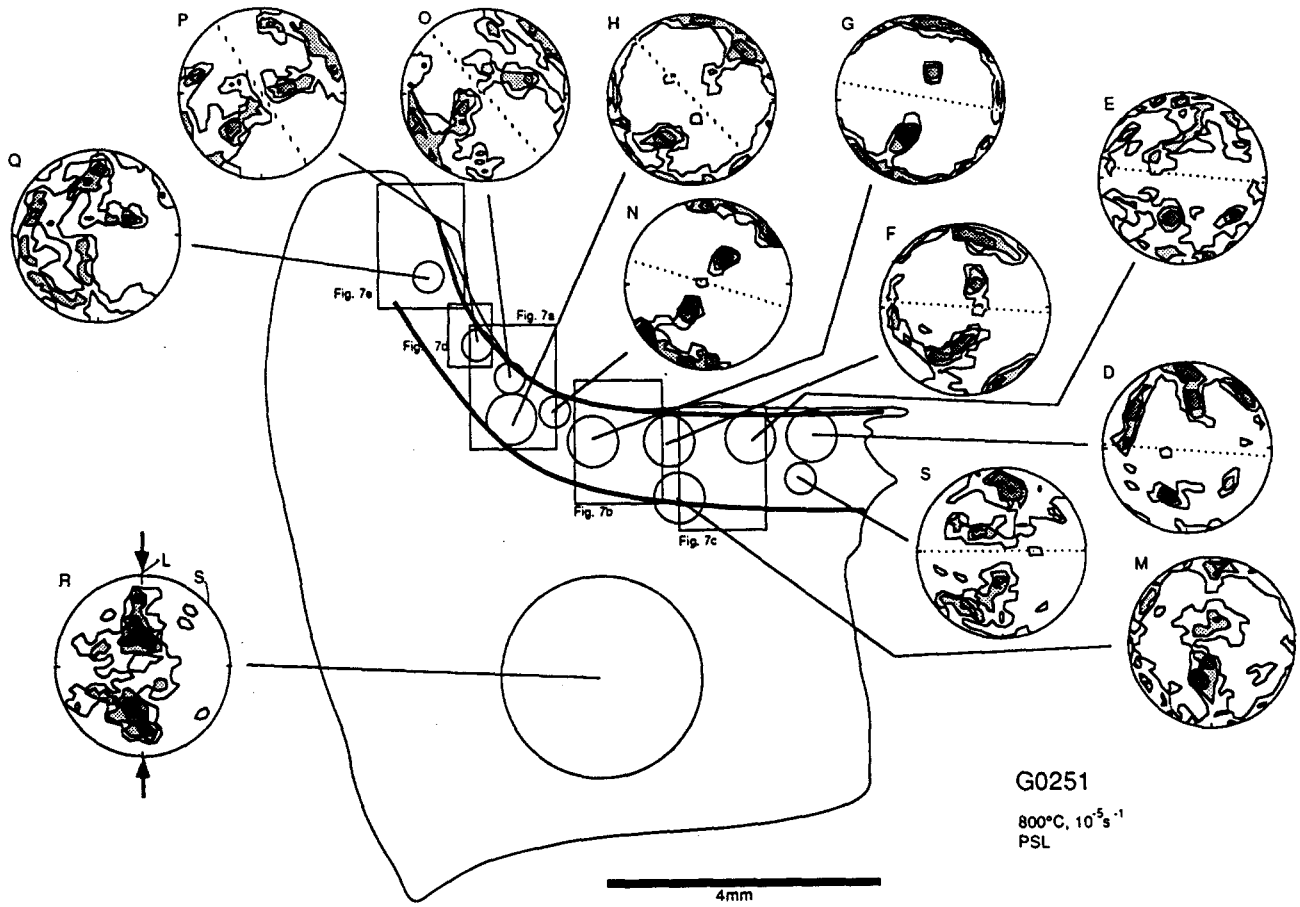

Fig. 12. *c*-axis fabrics developed in G0251 (PSL, 800°C, 10^{-6} s^{-1}, $\varepsilon = 57\%$). The measured areas are represented by the circles within the outline of the specimen section. The rectangles show the position of the photomicrographs in the specimen. The shear zone boundaries are indicated by the thick lines. Fabric R is measured in an area of low strain and gives an indication of the initial preferred orientation. *S* and *L* show the initial orientation of the foliation and lineation, respectively. The dotted line in the fabric diagrams indicates the orientation of the grain elongation. Contour interval 0.67,2,4 and 10% per 0.67% area, based on 150 orientations; equal-area projection.

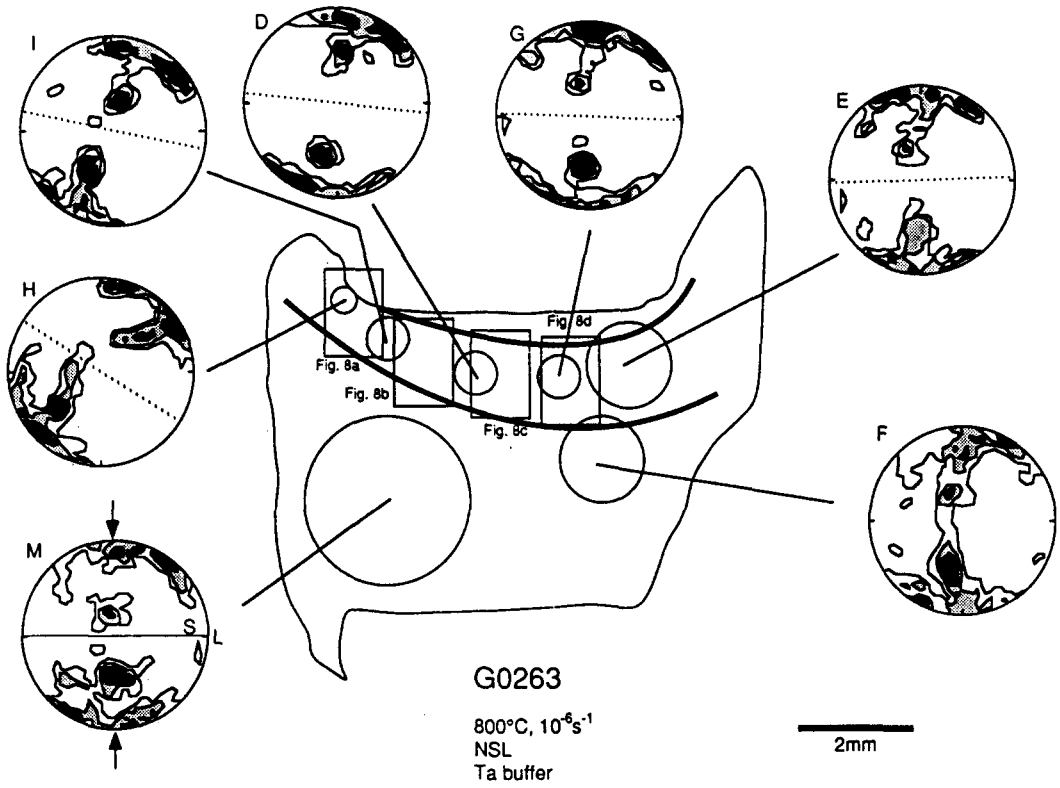

Fig. 13. *c*-axis fabrics developed in G0263 (NSL, 800°C, 10^{-6} s^{-1}, $\varepsilon \approx 57\%$). The shear zone boundaries are indicated by the thick lines. Fabric M is measured in an area of low strain and gives an indication of the initial preferred orientation. *S* and *L* indicate the initial orientation of the foliation and lineation respectively; arrows indicate the shortening direction. The dotted line in the fabric diagrams indicates the orientation of the grain elongation. Contour interval 0.67,2 and 4% per 0.67% area, based on 150 orientations; equal-area projection.

approximately 50° to the shortening direction in two of the shear zones in G0342 (Figs. 6a & c) indicates a higher shear strain. It is not possible to calculate the component of axial shortening accommodated in the shear zones.

Type B shear zones owe their origin to the geometry of the assembly. With increasing strain, the specimen begins to barrel and when the width of the specimen exceeds that of the piston, the piston punches into the specimen. This localizes deformation, allowing the specimen to shear past the piston corner. In some cases the zone showing a non-coaxial deformation history may extend under most of the piston (e.g. G0251, Fig. 7, G0263, Fig. 8). Only very small 'dead zones' are present under the pistons in these specimens. Shearing of the specimen past the piston corner allows movement of material within the 'dead zone'.

In specimen G0263 the distribution of the shear zones is asymmetric. Only a small portion of the deformed zones shows the foliation rotated anti-clockwise from the normal to the shortening direction (in the area where fabric E is measured, Fig. 12); most of the deformed zone has the foliation rotated clockwise (i.e. between fabrics G and H, Fig. 12). This asymmetry can be explained by examining the *c*-axis preferred orientation of the initial quartz mylonite (similar to fabric M, Fig. 12). This preferred orientation shows a maximum of *c*-axes approximately normal to the foliation developed in the shear zone, with the foliation rotated clockwise from the normal to the shortening direction (i.e. maximum clockwise from the girdle normal to the initial mylonitic foliation and linea-

Grains with *c*-axes in this orientation will deform easily by basal slip in an ⟨*a*⟩ direction, allowing formation of the shear zone. Few grains in the initial quartz mylonite have *c*-axes anticlockwise from the girdle normal to the initial mylonitic foliation and lineation. Formation of a shear zone anti-clockwise from the normal to the shortening direction is consequently much more difficult.

Strain history

The strain history in the two types of shear zones differs. In Type A shear zones, the shear zones are initially weak with respect to the host rock. At low strains the imposed shortening will be predominantly taken up by simple shear in these zones. This is indicated by the limited strain observed in the host rock (e.g. G0297, shortened 27%, Figs. 5a & b). As the total strain on the specimen is increased, more of the strain is accommodated in the host rock. This suggests that a later component of flattening overprints the shear zones. This may explain the *c*-axis maximum observed parallel to the shortening direction. It is not possible to calculate the component of flattening normal to the shear zone boundary (cf. normal strain calculated by Dell'Angelo & Tullis 1989).

In Type B shear zones the strain history is more complex. There is initial flattening of the specimen. The specimen is not sheared past the corner of the piston until there is a significant concentration of strain at the corner. This may not occur until shortening of at least

20–30% (no such shear zone is observed in G0297, shortened 27%). The strain path is then changed from one of flattening to one dominated by shear where the specimen is sheared past the corner of the piston. This is well illustrated in G0342, where flattened grains to the side of the piston can be followed into elongate grains which have been sheared past the piston corner (Fig. 9). The state of strain varies from one dominated by shear near the piston corner to one dominated by axial flattening under the piston, where the foliation is normal to the shortening direction. The strain history is more complex up the side of the piston (see microstructures, Fig. 7e and fabric Q, developed in G0251, Fig. 12), where there will be a decrease in temperature. The deformation conditions in this area are not well constrained and therefore no interpretation of this microstructure and preferred orientation will be given.

c-*axis preferred orientations*

The *c*-axis preferred orientations that develop in all areas showing a non-coaxial deformation history are similar to those observed within shear zones in the Earth's crust. They show well defined girdles approximately normal to the shape fabric.

The deformed, elongate nature of both original and recrystallized grains within the shear zones, the presence of deformation lamellae in the large relict grains both within and outside the shear zones, and the strong crystallographic preferred orientation normal to the shape fabric, all indicate that dislocation creep is the primary deformation mechanism within the areas showing a non-coaxial deformation history. However, it is not possible to delineate clearly the operating slip systems within the observed shear zones without TEM analysis. If the analyses of Schmid & Casey (1986) are used as a guide, they indicate that basal slip dominates. This is indicated by the presence of a strong *c*-axis maximum approximately normal to the foliation. The maxima in the girdle result from the interaction of basal, prism, and rhomb slip, all in an ⟨*a*⟩ direction. Alternatively, Dell'Angelo & Tullis (1989) suggest that such fabrics form by kinking on basal planes and basal slip.

Although the predominant feature of the fabrics is a girdle normal to the foliation, nearly all show a maximum parallel to the shortening direction (e.g. fabrics A,B,C in G0342, Fig. 10; fabrics F,G,H,N in G0251, Fig. 12; fabrics D,G,H,I in G0263, Fig. 13).

There may not be a unique mechanism of formation for this maximum parallel to the shortening direction in the specimens described. Two possibilities exist.

(a) Rotation of grains through the shortening direction. Grains which have *c*-axes located on the other side of the shortening direction from the normal to the shear zone foliation must rotate through the shortening direction to get into a stable orientation with respect to the deformation axes. This mechanism is best observed in G0263 (Fig. 13), in which a strong maximum is developed parallel to the shortening direction in the area where the foliation is normal to the shortening direction (fabric G). This maximum rotates clockwise along the shear zone (i.e. G→D→I→H). Grains with *c*-axes in this orientation will be deforming predominantly by basal slip, with basal planes rotating to remain approximately parallel to the foliation. The *c*-axis maxima in the fabrics in G0251 (Fig. 12) are also rotating in a similar manner to that described above (follow maxima which are normal to the foliation in fabrics E→F→G→N→H→P).

(b) Formation of *c*-axis maxima due to later flattening. Previous experimental studies (e.g. Tullis *et al.* 1973) show that *c*-axes rotate towards the shortening direction with increasing strain, forming either a point maximum parallel to, or small circles about the shortening direction. If strain is no longer accommodated in the shear zones, continued shortening will cause *c*-axes in grains in the shear zones to rotate towards the shortening direction. This mechanism may explain the maxima developed approximately parallel to the shortening direction in G0342 (Fig. 10).

Shear sense and asymmetry

Previous studies (field, experimental and theoretical) have shown that for coaxial strain histories *c*-axis fabrics develop which are symmetric with respect to the foliation (i.e. small-circle girdles for uniaxial compression and cross girdles for plane strain; Tullis *et al.* 1973, Tullis 1977, Burg & Laurent 1978, Lister *et al.* 1978, Schmid & Casey 1986). However, with increasing shear strain, a smooth continuum exists from a Type II cross girdle (Lister 1977) through a kinked girdle to a single girdle approximately normal to the foliation (Burg & Laurent 1978, Schmid & Casey 1986). As the shear strain is increased the girdle becomes smoother. This is well illustrated in the fabrics measured in the regions of highest shear strain in the described specimens (fabric N in G0251, Fig. 12). At lower shear strains in this specimen (as in other specimens) the girdles show a more kinked appearance (e.g. fabric F in G0251, Fig. 12).

In general, the sense of asymmetry of the *c*-axis girdle with respect to both the shape fabric and the shear zone boundary can be used to determine the sense of shear. The complex strain history, coupled with the initially strong crystallographic preferred orientation makes it difficult to interpret the asymmetry in the *c*-axis fabrics developed in the specimens described in this paper. In many of the measured fabrics the asymmetry can be attributed to the strong initial fabric (e.g. specimen G0263, Fig. 13). This is, however, not always the case, particularly for the fabrics in G0251 (Fig. 12) and G0342 (Fig. 10).

In G0251, in areas where a coaxial deformation history dominates, a symmetric fabric is developed with respect to the shape fabric (e.g. fabrics D,E,F,M, Fig. 12). Whereas the deformation history is non-coaxial, along the shear zone, the developed fabric shows an asymmetric distribution with respect to the shape fabric (e.g. fabrics G,N,O, Fig. 12). The sense of the asymmetry is a leading edge (Fig. 11) with respect to the sense

of shear. In G0342 the dominant feature is a girdle normal to the shape fabric. If the shear zone boundary is used as a reference in these shear zones the asymmetry in three of the girdles is trailing edge with respect to the sense of shear (Figs. 10a–c). However, it is not known to what extent later coaxial deformation contributes to this maximum, which in all cases is approxiamtely parallel to the shortening direction.

CONCLUSIONS

Two types of shear zones which formed in specimens of an experimentally deformed quartz mylonite have been described. One of these is discrete and cuts through the specimen, forming along cracks produced during pressurization. The other develops around the corner of the piston, where it has punched into the specimen. The microstructures in both types of shear zone are characterized optically by elongate grains defining a shape fabric which is not normal to the shortening direction. In the discrete shear zones (Type A shear zones) these grains are recrystallized. In the Type B shear zones, developed around the piston corners, elongate grains are both old ribbon-shaped grains and recrystallized grains.

The deformation histories of the two types of shear zones differ. In the discrete shear zones the strain history is initially dominated by shear (with the component of flattening normal to the shear zone unknown), followed by axial flattening at higher sample strains, when the shear zones may cease movement. The shear zones developed at the piston corners show initial flattening (to 20–30% shortening), followed by shearing past the corner of the specimen.

The *c*-axis preferred orientations which develop are similar in all shear zones, namely a girdle approximately normal to the shape fabric defined by the grain elongation. The sense of asymmetry in many of the preferred orientations can be attributed to the use of a mylonite as the starting material, showing a strong preferred orientation. This often shows an asymmetry which is a trailing edge with respect to the sense of shear, using the shear zone boundary as a reference plane. In one specimen there is not an initial asymmetric preferred orientation, and the asymmetry which develops in the shear zone is a leading edge with respect to the shear sense, again using the shape fabric as a reference plane.

The results obtained in these experiments suggests that some care is needed in interpreting *c*-axis preferred orientations in natural shear zones, especially if it is believed that the shear zone protolith had an initially strong preferred orientation. The asymmetry of the preferred orientation with respect to the shape fabric may be opposite to what one would normally expect. Therefore, it is important to use all available kinematic indicators to determine the sense of shear, and not rely solely on the *c*-axis preferred orientation.

Acknowledgements—The experiments described in this paper constitute a portion of a Ph.D. thesis completed at Monash University. The award of a Monash Graduate Scholarship is gratefully acknowledged. Bruce Hobbs and Alison Ord are thanked for guidance in things experimental, many useful discussions throughout the course of the project, and reading the chapter of the thesis that this paper is based on. Paul Williams and Laurel Goodwin are thanked for critical reading of this paper. The mechanical workshop at Monash, under the direction of Les Jones, and Alan White at CSIRO Division of Geomechanics are thanked for keeping the experimental rigs in working order, and constructing the intricate assemblies required for such a project. Robert Douglas at Monash University is thanked for producing many thin sections, often from difficult specimens. Graham Price is thanked for help with the photometer, and many useful discussions. Bob McCulloch is thanked for photographic work. The use of facilities at both Monash University and CSIRO, Division of Geomechanics is gratefully acknowledged. Critical reviews by E. Rutter and an anonymous reviewer are appreciated for clarifying many of the points presented in this paper, especially concerning the formation of the shear zones.

REFERENCES

Bouchez, J.-L. & Pêcher, A. 1978. The Himalayan Main Central Thrust pile and its quartz-rich tectonites in central Nepal. *Tectonophysics* **78**, 23–50.

Burg, J.-P. & Laurent, P. 1978. Strain analysis of a shear zone in a granodiorite. *Tectonophysics* **47**, 15–42.

Dell'Angelo, L. N. & Tullis, J. 1989. Fabric development in experimentally sheared quartzites. *Tectonophysics* **169**, 1–21.

Friedman, M. & Higgs, N. G. 1981. Calcite fabrics in experimental shear zones. In: *Mechanical Behaviour of Crustal Rocks. The Handin Volume* (edited by Carter, N. L., Friedman, M., Logan, J. M. & Stearns, D. W.). *Am. Geophys. Un. Geophys. Monogr.* **24**, 11–27.

Kern, H. & Wenk, H.-R. 1983. Calcite texture development in experimentally induced ductile shear zones. *Contr. Miner. Petrol.* **83**, 231–236.

Lister, G. S. 1977. Discussion: Crossed-girdle *c*-axis fabrics in quartzites plastically deformed by plane strain and progressive simple shear. *Tectonophysics* **39**, 51–54.

Lister, G. S., Paterson, M. S. & Hobbs, B. E. 1978. The simulation of fabric development in plastic deformation and its application to quartzite: the model. *Tectonophysics* **45**, 107–158.

Ord, A. & Hobbs, B. E. 1986. Experimental control of the water-weakening effect in quartz. In: *Mineral and Rock Deformation: Laboratory Studies. The Paterson Volume.* (edited by Hobbs, B. E. & Heard, H. C.). *Am. Geophys. Un. Geophys. Monogr.* **36**, 51–72.

Price, G. P. 1979. The analysis of quartz *c*-axis fabrics by the photometric method. *J. Geol.* **88**, 85–100.

Price, G. P. 1985. Preferred orientations in quartzites. In: *Preferred Orientation in Deformed Metals and Rocks: An Introduction to Modern Texture Analysis* (edited by Wenk, H.-R.). Academic Press, New York, 385–406.

Ralser, S. 1987. Experimental deformation of a quartz mylonite. Unpublished Ph.D. thesis, University of Monash.

Ralser, S., Hobbs, B. E. & Ord, A. 1987. Experimental deformation of a quartz mylonite: The effect of orientation. In: *Int. Conf. Deformation of Crustal Rocks. Geol. Soc. Aust. Abs.* **19**, 82–83.

Ramsay, J. G. 1980. Shear zone geometry: a review. *J. Struct. Geol.* **2**, 83–99.

Ramsay, J. G. 1983. Rock ductility and its influence on the development of tectonic structures in mountain belts. In: *Mountain Building Processes* (edited by Hsü, K. J.). Academic Press, New York, 111–127.

Rutter, E. H. & Rusbridge, M. 1977. The effect of non-coaxial strain paths on crystallographic preferred orientation development in the experimental deformation of marble. *Tectonophysics* **39**, 73–86.

Schmid, S. M. 1983. Microfabric studies as indicators of deformation mechanisms and flow laws operative in mountain building. In: *Mountain Building Processes* (edited by Hsü, K. J.). Academic Press, New York, 95–110.

Schmid, S. M. & Casey, M. 1986. Complete texture analysis of commonly observed quartz *c*-axis patterns. In: *Mineral and Rock Deformation: Laboratory Studies. The Paterson Volume* (edited by

Hobbs, B. E. & Heard, H. C.). *Am. Geophys. Un. Geophys. Monogr.* **36**, 263–286.
Schmid, S. M., Panozzo, R. & Bauer, S. 1987. Simple shear experiments on calcite rocks: rheology and microfabric. *J. Struct. Geol.* **9**, 747–778.
Tullis, J. 1977. Preferred orientation of quartz produced by slip during plane strain. *Tectonophysics* **39**, 87–102.
Tullis, J. A., Christie, J. M. & Griggs, D. T. 1973. Microstructures and preferred orientations of experimentally deformed quartzites. *Bull. geol. Soc. Am.* **84**, 297–314.